Prediction and Tracking Analysis of a Class of High Area-to-mass Ratio Debris Objects in Geosynchronous Orbit*

Tom Kelecy
Boeing LTS, Colorado Springs, CO / Kihei, HI

Edwin S. Barker
NASA/Johnson Space Center, Orbital Debris Program Office, Houston, TX

Patrick Seitzer
The University of Michigan, Ann Arbor, MI

Tim Payne
Air Force Space Command / A9AC, Colorado Springs, CO

Robin Thurston
614 AOC/OL-B, Colorado Springs, CO

ABSTRACT

A subset of the population of deep space objects is thought to be high area-to-mass ratio (A/m) debris having origins from sources within the geosynchronous orbit (GEO) belt. The typical A/m values for these have been observed to range anywhere from 1's to 10's of m^2/kg, and hence, are susceptible to significant solar radiation pressure effects which result in long-term migration of eccentricity (0.1-0.6) and inclination over time. However, the nature of the debris orientation-dependent dynamics also results time-varying solar radiation forces about an average value over shorter time scales which complicate the short-term orbit determination (OD) processing and prediction. In November of 2007, several of these objects were acquired and tracked from the 0.9 m telescope at the Cerro Tololo Inter-American Observatory (CTIO) in Chile using prediction products derived from the orbit determination of optical angles tracking data. The estimated states computed using the Orbit Determination Tool Kit (ODTK) included dynamic estimation of the area-to-mass ratio, the variations of A/m relative to an average value. The work presented in this paper assesses the OD, prediction and tracking performance using the ODTK derived predictive products that were utilized during the survey, the CTIO tracking data that was collected, and the post-fit orbit products resulting from additional data collected after the observations. The OD and A/m estimation performance for a selected object tracked is presented, and the derived prediction performance is also analyzed by comparison with the CTIO 0.9 m telescope acquisition metrics. The post-fit prediction assessments of 10's of kilometers positional accuracy over 24-48 hour prediction spans is consistent with the arc-minute level tracking offsets that were observed.

1. BACKGROUND AND MOTIVATION

Background

Schildknecht, et al.[1] discovered a population of deep space objects is thought to be debris having origins from sources in the geosynchronous orbit (GEO) belt. There is a heightened interest in the international space community due to the large number and small size of these objects, as they pose a hazard to active satellites operating in the vicinity of the GEO belt. The longitudinal migration due to orbit perturbations, along with the dimness and variability of the visual magnitudes make them a challenge to track consistently. Their apparent small size makes this debris a dim optical target, and at GEO ranges, nearly impossible to track with radar. Nevertheless, repeat tracking is paramount to making long-term observations with other sensors that will allow better characterization of

* Distribution A: Approved for public release; distribution unlimited.

the material makeup of these objects, and provide long-term orbital histories that might allow the debris to be tied to specific breakup events or objects of origin.

Analysis has been conducted[1,2,3] indicating that these objects have area-to-mass ratios (A/m's) averaging anywhere from 1's to 10's of m^2/kg, and thus explains observed migration of eccentricity (0.1-0.6) and inclination that distinguishes their orbital characteristics. The solar radiation pressure (SRP) perturbation effects on orbital period, inclination and eccentricity can vary significantly over relatively short periods of time. The amplitudes and periods of the perturbations vary according to the A/m.

Collecting photometric measurements is necessary to support characterization of the material make-up and size of the debris. Hence, the collection of measurements over time requires tracking and orbit determination (OD) that supports re-acquisition of specific debris objects. The work presented in this paper summarizes the orbit analysis and prediction of one particular debris object for which tracking measurements are available. These results are used as a reference for the analysis of the metric data collected by NASA on the 0.9 m telescope located in Chile to assess acquisition and tracking performance.

2. TRACKING DATA HISTORY AND ORBIT DETERMINATION PROCESSING

Numerous high area-to-mass ratio (A/m) debris objects are tracked by various networks (U.S. Air Force Space Command (AFSPC), NASA and the European Space Agency (ESA)). One of these objects was chosen for the subject of this analysis. The object has an A/m = 3.4 m^2/kg, a nominal semi-major axis of a = 42,449.5 km, inclination of i = 15.8 deg, and an eccentricity of e = 0.093. Optical Right Ascension (RA) and Declination (Dec) measurements were available for most of 2007 from available tracking data, which included metrics from a series of observations conducted from Chile in November of 2007. This long data span permitted orbit determination and prediction analysis to be performed.

An OD process was developed to provide high A/m object tracking and prediction products that could be used to support acquisition and tracking campaigns by international collaborators. The orbital dynamics result in observation phasing that truly requires continuous global coverage to insure that the objects are not "lost." The estimated state consists of position and velocity information, and a solar radiation pressure coefficient "factor" that effectively estimates a measure of the area-to-mass ratio. The consistent tracking coverage assures consistent measurements that can be used to characterize the object properties and orientation-dependent dynamics.

The Orbit Determination Tool Kit (ODTK) was used to process a "real-time" implementation of the state estimation[5]. ODTK utilizes a Kalman filter based approach to the estimation, and so a state estimate is provided at each measurement update, hence, a time history of each estimated parameter is available. This includes the capability to provide SRP estimates with each measurement update and, hence, to provide insight into the A/m dynamics that might occur over a data series, and also to improve the orbit estimates. In particular, the potential time variability of the *A/m* parameter is of interest. Furthermore, the filtered state can be smoothed "backwards" over a specified data span to provide an optimal state estimate that reduces the uncertainty over that produced by the real-time filter. The filter parameters are saved after the latest update, and so after a measurement outage, the state is automatically propagated to the new measurement time, and proceeds with the filter update as long as data from a pass is available. Most noteworthy is that the ODTK Kalman filter implementation allows A/m to be estimated with each measurement update, and so characterization of the time history is possible. This will be demonstrated in the results presented in the following sections.

The OD analysis follows the process depicted in Fig. 1 which is summarized as follows:

1. Perform the initial orbit determination and/or initial least-squares to determine the initial state
2. Do an initial filter/smoother pass through data with high a priori state covariance, and where needed, dynamic measurement editing
3. Examine residuals, position consistency, and A/m average estimate, and revise filter covariance and editing parameters as appropriate
4. Adjust A/m and associated sigma's, including ecliptic north and ecliptic plane fractions, and re-run the filter/smoother

5. When the A/m estimate is stable, update initial position and velocity state and covariance with the smoother state estimate, and re-run
6. Determine A/m average, variability, position consistency and error growth over data gaps

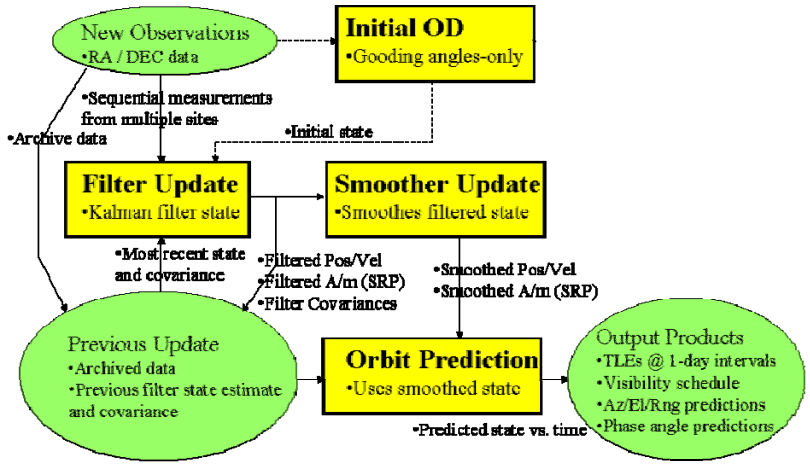

Fig. 1 ODTK Orbit Determination Processing

The Kalman filter processing produces a state estimate, or, an estimate of the position, velocity and solar radiation pressure (SRP) for the tracked object. A comparison of the estimates for the processed debris object tracking data over most of 2007 produces the a posteriori measurement residuals, shown in Fig. 2. The measurement residuals have variations on the order of several arc-seconds which is the expected noise level of the optical data. Noteworthy are several data outages, some as long as several weeks, which result from loss of visibility as the object migrates into and out of view of various sensors.

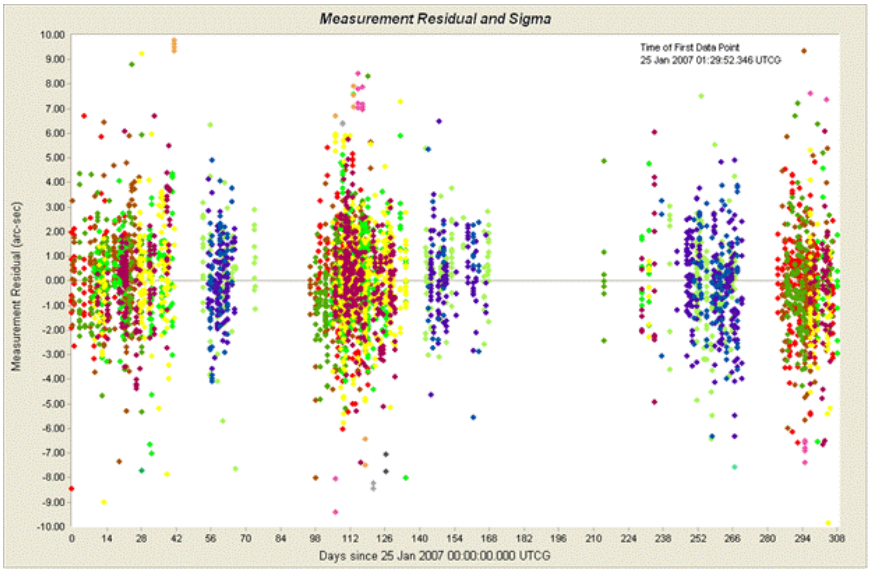

Fig. 2 Debris Object Measurement Residuals

The Kalman filter process provides a state estimate at each measurement update time. In between measurements, the last known state is propagated from the last measurement to the next measurement. The estimation covariance, a measure of the state uncertainty, is concurrently propagated with the state. The radial (blue line), along-track (red line) and cross-track (black line) σ's derived from the covariance are plotted in Fig. 3 for the period. The state uncertainty is on the order of several kilometers where data are available, but grows to several hundred kilometers during data outages. Most of the error develops in the along-track direction, likely due to weaker observation

geometry in the radial direction from the optical measurements. This would be more than enough error for some sensors to "lose track" of the object if inadequate tracking coverage is available.

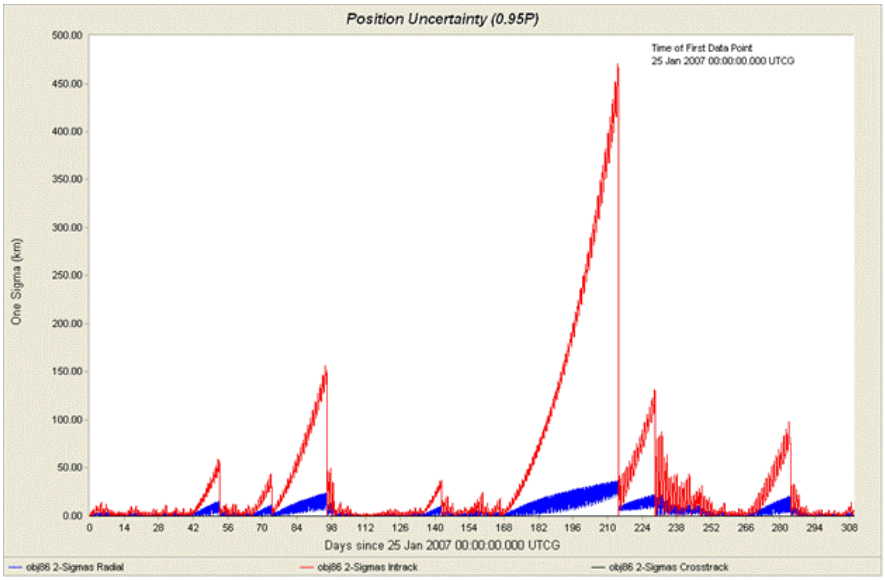

Fig. 3 Debris Object Filtered RAC Position Uncertainties

The filter estimates can be post-processed by a back smoothing process which takes advantage of all of the available data and the filter uncertainties. Its purpose is to "smooth" any physically un-natural changes in the state that might occur during a measurement update in the Kalman filter. The smoothed RIC uncertainties for the object over the period are given in Fig. 4, where again one can see the increase in uncertainty where no observations were available. However, the over-all magnitude of the estimation uncertainties is drastically reduced for the smoother estimates, the result of the additional information gained through the post-processing. This is equivalent to batch least-squares processing, but with the added advantage of retaining the dynamics of the estimated parameters.

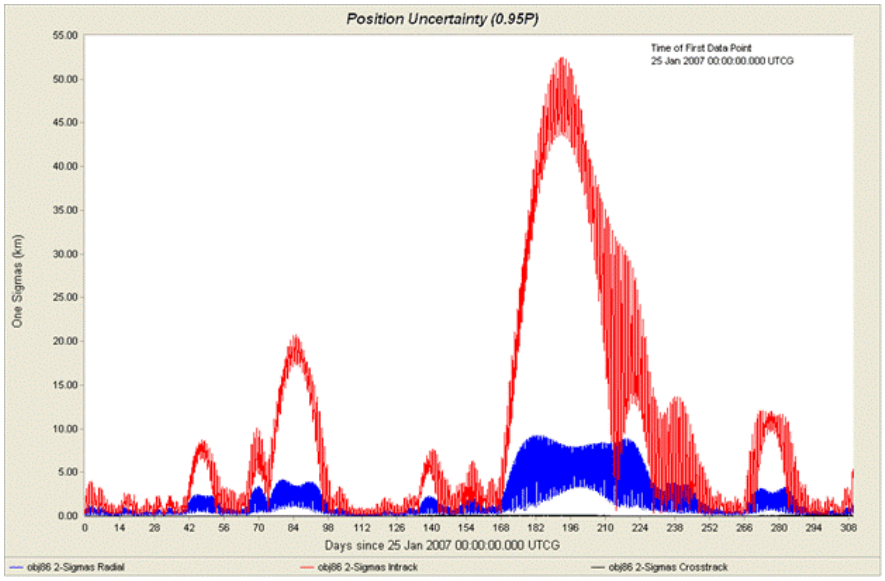

Fig. 4 Debris Object Smoother RAC Position Uncertainties

In addition to earth, lunar and solar gravitation, the solar radiation pressure (SRP) is a significant force affecting the orbital dynamics of high A/m GEO objects. The solar radiation acceleration is[6]

$$\bar{a}_{radiation} = \frac{p_{SR} c_R A_S}{m} \hat{r}_S \tag{1}$$

where

p_{SR} = solar radiation pressure

c_R = solar pressure parameter

A_S = effective area facing sun

m = object mass

$\hat{r}_S$ = vector from object to sun

In most OD implementations a nominal value of c_R is typically specified, and a fixed correction estimated as part of the batch least squares state solution. The values of A_S and m are usually specified if those properties are known, and the values of p_{SR} and $\hat{r}_S$ are computed based on the orbital geometry relative to the sun. In the absence of physical information of the object properties, the combined quantity of

$$\gamma = \frac{c_R A_S}{m} \tag{2}$$

can be estimated. If c_R is assumed to be equal to 1, then the OD process is effectively estimating A_S/m. Note that mass is assumed fixed, and so A_S/m variations are really just an indication of the object orientation changes resulting in variation of the cross sectional area exposed to the sun. All discussions of A/m throughout this work are taken to be synonymous with SRP.

The filtered A/m estimated for the debris object is shown in Fig. 5, and the corresponding smoothed estimate in Fig. 6. These represent the A/m corrections at each measurement update relative to the average value of A/m = 3.4 m^2/kg. The variation in both filtered and smoothed estimates each have a near 0.1 m^2/kg, and in this case, there is no obvious periodicity in these variations. As shall be demonstrated later in this paper, the variations can have an impact on the prediction accuracy.

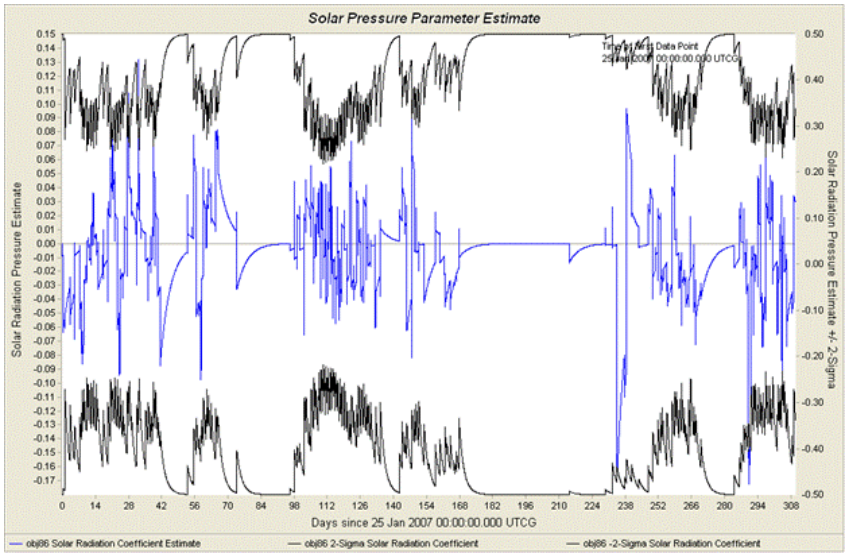

Fig. 5 Debris Object Filtered SRP (A/m) Estimates

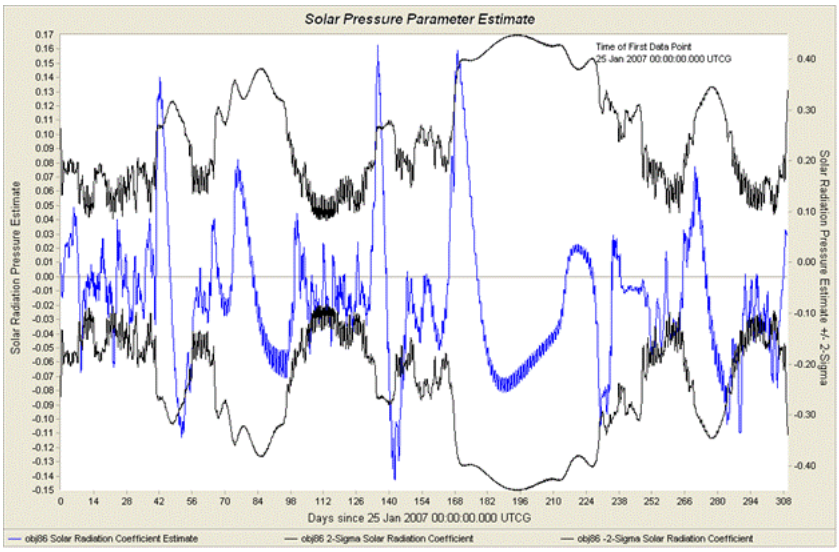

Fig. 6 Debris Object Smoother SRP (A/m) Estimates

The performance of the Kalman filter estimates, and the subsequent smoothing of the filter solutions, can be measured according to the consistency of the measurement corrections relative to the updated covariance. A measure of filter-smoother performance, known as the "McReynolds' consistency test", can be summarized by defining the following[7]:

$$X_k^f = \text{filtered state estimate at time } t_k$$

$$X_k^s = \text{smoother state estimate at time } t_k$$

$$P_k^f = \text{filtered covariance estimate at time } t_k$$

$$P_k^s = \text{smoother covariance estimate at time } t_k$$

then compute the estimated state and covariance differences between the filter and smoother:

$$X_{\Delta k} = X_k^f - X_k^s \tag{3}$$

$$P_{\Delta k} = P_k^f - P_k^s \tag{4}$$

Then for, the i^{th} element of $X_{\Delta k}$ and the square root of the i^{th} element of $P_{\Delta k}$ (sigma symbol) define the ratio

$$R_k^i = \frac{X_{\Delta k}^i}{\sigma_{\Delta k}^i} \tag{5}$$

If abs(R_k^i) ≤ 3 for all i and k, then the test is satisfied globally for each estimate. If abs(R_k^i) > 3 for all i and k, then the filter-smoother test fails globally indicating the possibility of modeling inconsistencies. Thus, position, velocity and A/m estimation performance can be assessed in terms of the ratio of the estimates to the predicted/assumed modeling uncertainties.

The RAC position consistency values for the debris object estimates are shown in Fig. 7, where with the exception of a couple of anomalies, they are seen to be less than 3 indicating the solutions are consistent with the estimation uncertainties. Similarly, the SRP consistencies for those estimates are seen in Fig. 8 to also be less than 3. Previous work indicates there could be forces orthogonal to the sun-line[8,9] and, hence, the appropriate process noise models need to be incorporated to achieve consistency in the SRP estimate.

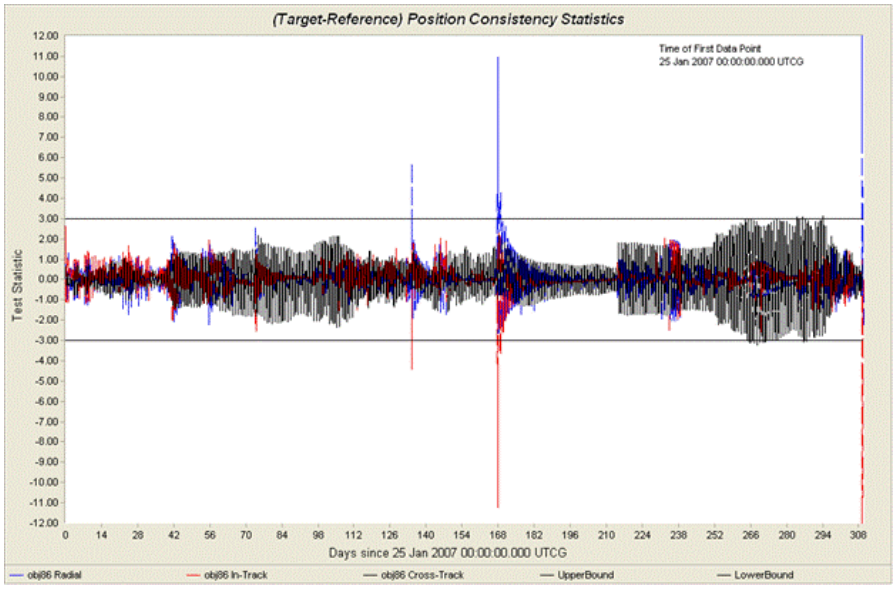

Fig. 7 Debris Object Filter-Smoother Position Consistency Test

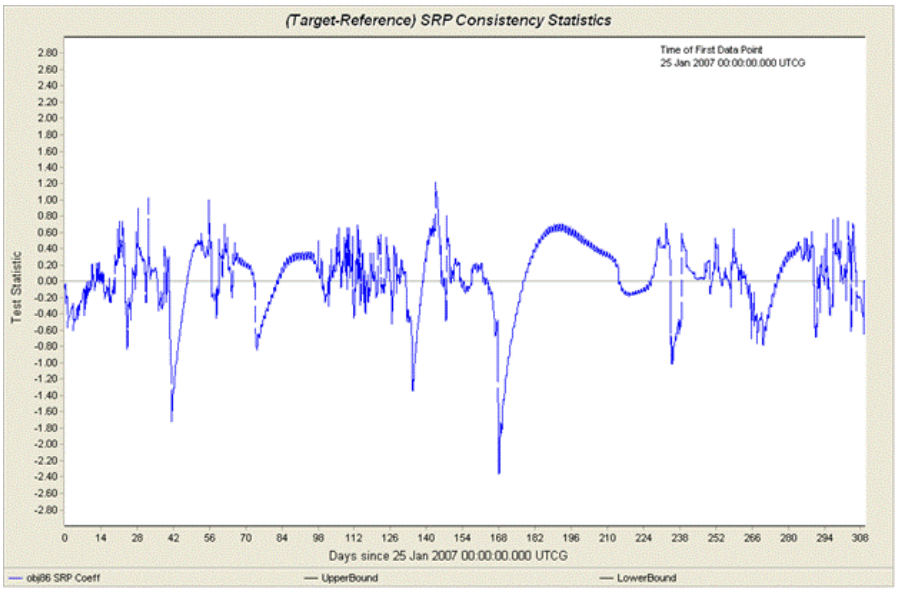

Fig. 8 Debris Object Filter-Smoother SRP (A/m) Consistency Test

3. CTIO C9 (0.9 m) DATA ANALYSYS

The CTIO C9 telescope (Fig. 9) was used to track several debris objects in an observing campaign conducted in November of 2007. The telescope is located at the Cerro Tololo Inter-American Observatory (CTIO) in La Serena, Chile. It is has 0.9 m Cassegrain optics, 0.792 arc-seconds per pixel, and a 13.2 arc-minute field-of-view (FOV). It has a blue sensitive CCD and is enlisted by NASA for approximately 4 weeks per year to support debris projects such as GEO high A/m observations.

Fig. 9 CTIO C9 (0.9 m) Telescope

Observations were collected on the debris object over the 4 days of November 13-16, 2007. The tracking was astrometrically reduced to provide RA and Dec pairs for the object, and these were compared to the independent "reference" orbit derived from the tracking data. These residuals are shown in Fig. 10, and represent the *a priori* residuals (no orbit adjustment applied). The residuals vary from several arc-seconds to several tens of arc-seconds relative to the reference. Post-fit residuals indicate the C9 data noise of less than an arc-second.

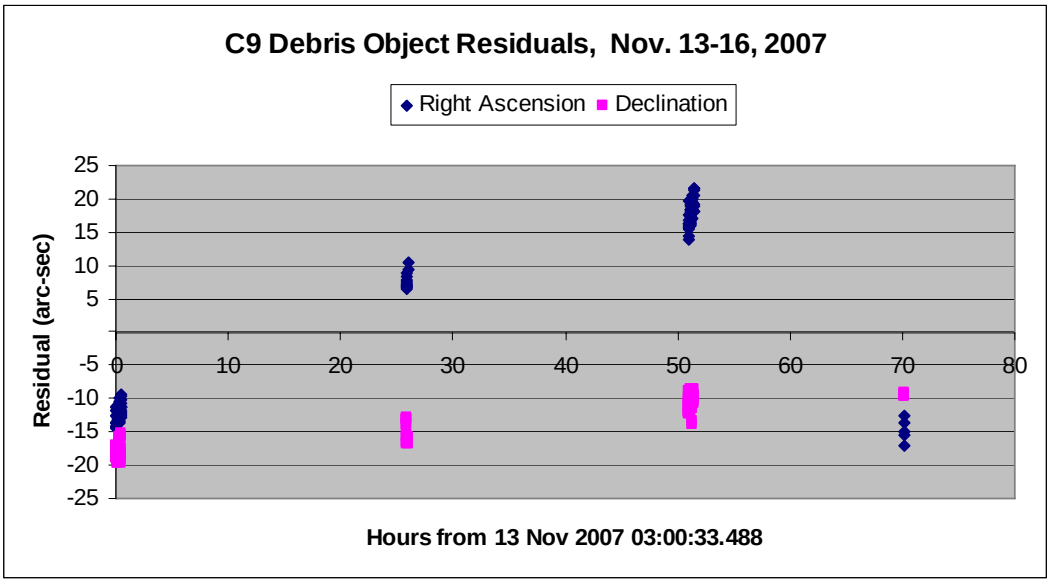

Fig. 10 CTIO C9 (0.9 m) Measurement Residuals vs. Tracking Derived Reference for Nov. 13-16, 2007

It is of interest to scale these *a priori* residuals to spatial errors at the range of the object. Table 1 shows the results of scaling the maximum residual errors of 20 arc-seconds to the minimum and maximum tracking ranges of 35400 *km* and 42300 *km*, respectively. It can be seen in the table that these errors 3.5-3 *km* spatial offsets. To corroborate

this, the C9 data was fit to an orbit, and that was compared to the independent reference orbit. The resulting RAC position differences, shown in Fig. 11, confirm orbital position differences on the order of several kilometers.

Table 1 CTIO C9 Pointing Errors for the Debris Object

Debris Object	Nov. 13-16, 2007		
Coordinate	Max Bias (arcsec)	Min Ptg Error (km)	Max Ptg Error (km)
Right Ascension	20	3.432	4.102
Declination	-20	-3.432	-4.102

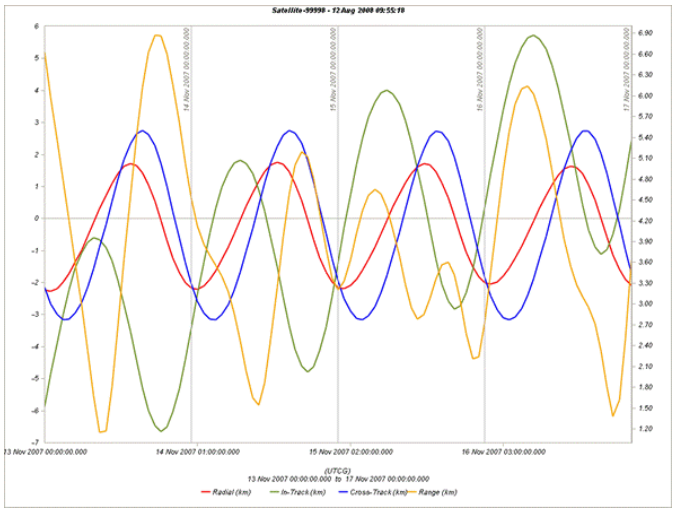

Fig. 11 C9 vs. Tracking Derived Orbit Differences for the Debris Object

These are certainly within the estimated position uncertainties that were shown in Figs. 3 and 4 for the reference orbit, as observation data for the reference over the period of comparison (Nov. 13-16) indicates uncertainties of a few kilometers. The RAC state differences shown in Fig. 12 also confirm this, where the period of comparison is represented at the far right end of the series. The conclusion is that the differences between the CTIO C9 data and the reference orbit are consistent to the level of the reference orbit uncertainty.

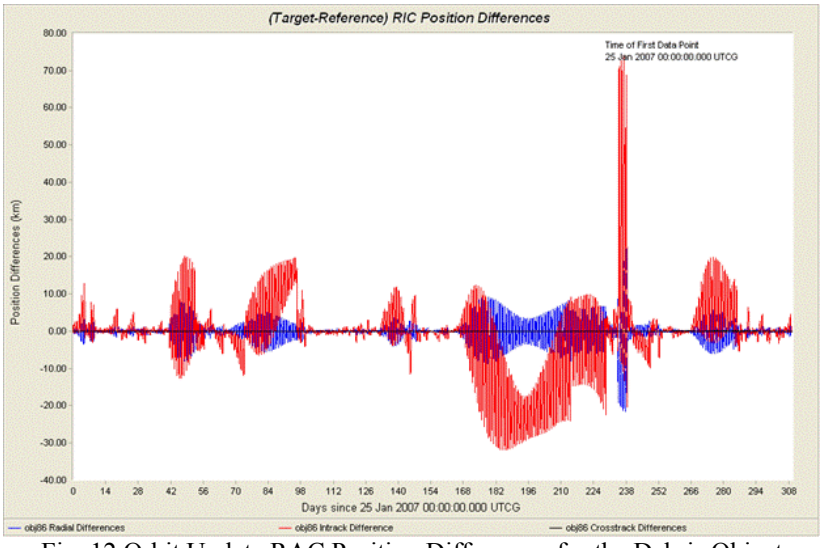

Fig. 12 Orbit Update RAC Position Differences for the Debris Object

However, it is suspected that there exists a small timing bias in the C9 measurement data. To estimate this bias, the along-track component of the orbit differences between the C9 and reference data (Fig. 11) was divided by the nominal "reference" orbit velocity. The result is shown in Fig. 13 for the period of Nov. 13-16, 2007. Though the estimated bias of several 10's of milliseconds is expected, the systematic error due to orbit uncertainties appears to dominate the profile.

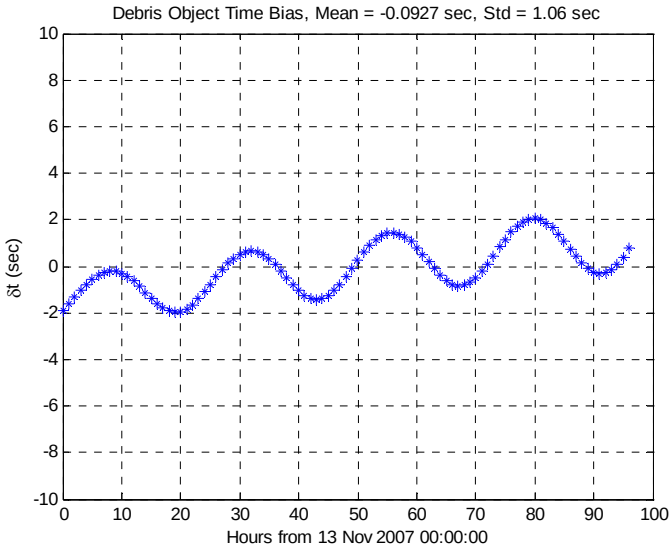

Fig. 13 CTIO C9 Measurement Timing Bias Estimates

4. HIGH A/M DEBRIS PREDICTION ERROR ANALYSIS

The acquisitions for the C9 observations were based on two-line element sets (TLEs) derived from the ODTK orbit solutions. The state solutions (position, velocity and SRP) at the most recent measurement updates were used as initial conditions for predictions through the acquisition period, and SGP4 fits to those resulting trajectories used to generate the acquisition TLEs. The trajectories were propagated using the force models and integrators internal to ODTK.

Since subsequent tracking data were acquired for the period of C9 observations, it is of interest to examine the expected acquisition accuracy as determined by a comparison of the predictions to the post-fit solutions. Table 2 presents a summary of the comparison of the derived TLE with respect to the post-fit (smoothed) orbit solutions over a period of 7 days in 1-day increments. The along-track error (the largest component) ranges from 10's to 100's of kilometers, with pointing errors shown which correspond to minimum, maximum and average tracking ranges of 25224 *km*, 42282 *km* and 40298 *km*, respectively. Those pointing errors grow from 7.1arc-minutes to 50.5 arc-minutes over the 7-day prediction span. The 13.2 arc-minute C9 FOV indicates the object predictions uncertainties would have pushed it out of view after only a day or two.

Table 2 TLE Predictions Derived from State Vectors

TLE Propagation Time (days)	Max Along-trk Error (km)	At Min Range (arcmin)	At Max Range (arcmin)	At Avg Range (arcmin)
1	83.0	8.1	6.7	7.1
2	167.2	16.3	13.6	14.3
3	250.1	24.4	20.3	21.3
4	337.5	32.9	27.4	28.8
5	422.6	41.2	34.4	36.1
6	507.4	49.5	41.3	43.3
7	592.2	57.8	48.1	50.5

The previous results represent an SGP4 fit to the predicted trajectory. What if the actual high fidelity trajectory were used instead? These results are shown in Table 3 where it can be seen that the resulting pointing errors do not exceed 0.59 arc-minutes after 7 days when compared to the post-process data. This is a significant (order-of-magnitude) improvement over the use of TLEs.

Table 3 State Vector (P,V, Nominal A/m) Predictions

State Propagation Time (days)	Max Along-trk Error (km)	At Min Range (arcmin)	At Max Range (arcmin)	At Avg Range (arcmin)
1	2.8	0.27	0.23	0.24
2	5.0	0.49	0.41	0.43
3	5.5	0.54	0.45	0.47
4	5.5	0.54	0.45	0.47
5	6.0	0.59	0.49	0.51
6	6.2	0.61	0.50	0.53
7	6.9	0.67	0.56	0.59

The trajectory prediction performance estimates summarized in Table 3 represent a prediction based on the "average" SRP value. However, we have seen that for this object the A/m can vary up to 0.1 m^2/kg or more. A trajectory was propagated with an A/m deviation of 0.1 m^2/kg and the result compared to the post-processed reference to assess the sensitivity to possible variations in A/m. The results, presented in Table 4, and depicted in Fig. 14, indicated a pointing error growth ranging from 0.49 arc-minutes to 2.89 arc-minutes over the 7-day prediction period, or over a 4-fold increase over the "average" trajectory. This 3% deviation is less than some of the A/m variations previously observed, so the variations to present a challenge to prediction and acquisition of these class of objects.

Table 4 State Vector (P,V, Perturbed A/m) Predictions

State Propagation Time (days)	Max Along-trk Error (km)	At Min Range (arcmin)	At Max Range (arcmin)	At Avg Range (arcmin)
1	5.8	0.57	0.47	0.49
2	10.6	1.03	0.86	0.90
3	15.1	1.47	1.23	1.29
4	20.3	1.98	1.65	1.73
5	25.3	2.47	2.06	2.16
6	29.6	2.89	2.41	2.53
7	33.9	3.31	2.76	2.89

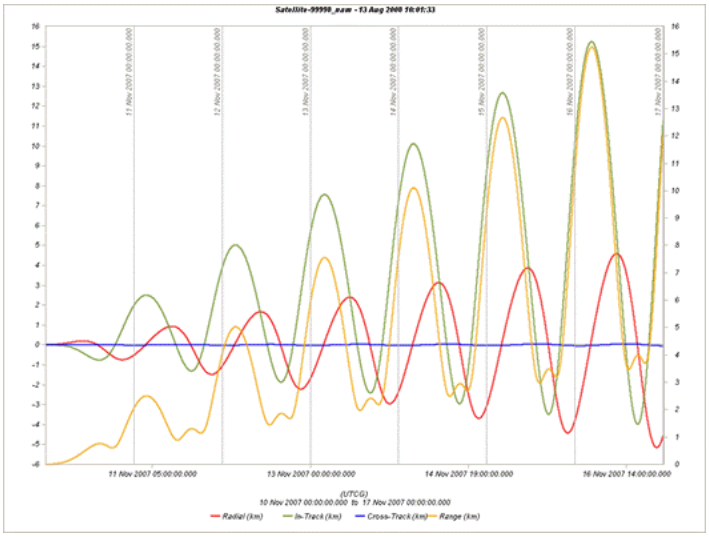

Fig. 14 Debris Object RAC Position Differences for Nominal vs. Perturbed SRP (A/m)

5. CONCLUSIONS AND FUTURE WORK

The orbit determination and prediction performance were analyzed in detail for a high A/m debris object using optical tracking data. The Orbit Determination Tool Kit was used for the OD and prediction. This "reference" orbit was also used to assess the quality of metric data derived from the CTIO C9 telescope.

It was seen that the OD performance for optical data is on the order of kilometer level or better in position, and a resulting along-track error growth of as much as 10 *km/day*. The C9 data quality was seen to have noise less than an arc-second, and subsequent orbit fit appears to be of comparable quality of the reference orbit. However, a possible timing bias might be affecting the quality of the solutions. Other sources of error that need to be explored are possible site coordinate errors, and minor coordinate frame incompatibilities.

Using the post-processed orbit solutions as a reference, the predictions using the TLE as a basis for acquisition indicates quality sufficient to support predictions out to 1-2 days. Use of the state vector and high fidelity force models extends the quality to a week, and possibly well beyond. Finally, the variations in A/m can inject significant error into the predictions, and reduce the accuracy by a factor of 4.

Future work will include more acquisition support for debris observations, and possibly support of hand-off exercises and collaboration with ESA in tracking and observing. An in-depth analysis into assessing the sensitivity of predictions to A/m variations is warranted. It might also prove worthwhile to incorporate time-varying models into predictions where appropriate. These analyses would be conducted through a combination of simulation and actual data analysis.

6. ACKNOWLEDGEMENTS

We would like to acknowledge the NASA Orbital Debris Program Office for supporting the analysis presented here and Dick Hujsak at AGI for ODTK consulting support.

7. REFERENCES

1. Schildknecht, et al., "Properties of the High Area-to-mass Ratio Space Debris Population in GEO," AMOS Tech. Conf., Sept, 2005.
2. Liou, J.-C., and Weaver, J. K., "Orbital Evolution of GEO debris with very high area-to-mass ratios", ODQN, Vol. 8, Issue 3, 2004.
3. Anselmo, Luciano and Carmen Pardini, "Long-Term Simulation of Objects in High-Earth Orbits," Space Flight Dynamics Laboratory, Pisa, Italy, ESA/ESOC Contract to ISTI/CNR Report, Contract No. 18423/04/D/HK, 13 December, 2006.
4. Liou, J.-C., and Weaver, J.K. , "Orbital dynamics of high area-to-mass ratio debris and their distribution in the geosynchronous region." In 4th European Conference on Space Debris, ESA publication SP-587, pp 285-290, 2005.
5. Hujsak, Richard S., James W. Woodburn, John H. Seago, "The Orbit Determination Tool Kit (ODTK) – Version 5," AAS 07-125, AAS Astrodynamics Specialist Conference, Mackinac Island, MI, August 2007.
6. Vallado, David A., "Fundamentals of Astrodynamics," Second Edition, Microcosm Press, 2001.
7. Wright, James, "Optimal Orbit Determination," Analytical Graphics, Inc., internal white paper, 2002.
8. Kelecy, Tom, Ray Deiotte, John Africano, Tim Payne and Gene Stansbery, "Orbit Processing and Analysis of a GEO Class of High Area-to-mass Ratio Debris Objects," AMOS Tech. Conf., Sept., 2006.
9. Kelecy, Tom, Tim Payne, Robin Thurston and Gene Stansbery, "Solar Radiation Pressure Estimation and Analysis of a GEO Class of High Area-to-mass Ratio Debris Objects", AAS 07-391, AAS Astrodynamics Specialist Conference, Mackinac Island, MI, August 2007.